# Modeling the Temperature Field in Reforming Anodes of a Button SOFC

I. Zinovik*, D. Poulikakos**

* Swiss Federal Institute of Technology, D-MAVT, LTNT
ML J27.1, Zuirch 8092, Switzerland, izinovik@ethz.ch
** Swiss Federal Institute of Technology, D-MAVT, LTNT
ML J36, Zurich 8092, Switzerland, dimos.poulikakos@sl.ethz.ch

## ABSTRACT

A new model to simulate temperature distribution in porous reforming anodes of SOFCs is suggested. The model is implemented in a commercial CFD software package. Heat transfer, fluid flow and electrochemical reactions are simulated within a button SOFC studied in the experiments. The model is applied to investigate temperature gradients and reactive flow in graded anodes composed of multiple layers.

The modeling effort aims to provide to cleantechnology a comprehensive simulation platform for study of the reactive flow in SOFCs. The simulations allow for an insight into the electrochemical transport processes in micro-scale porous structure. The modeling can be a valuable alternative to expensive experiments and play a crucial role in fuel cell optimization especially when the measurements are not readily available.

***Keywords***: sofc, methane, reforming anode, cfd

## 1 INTRODUCTION

In recent years, one of the trends in the development of commercially feasible solid oxide fuel cells (SOFC) is a replacement of pure hydrogen fuel by various hydrocarbon mixtures. The advantages of using hydrocarbon fuels include better energy conversion efficiency. For example, our experiments show that the porous catalytic layers boost the conversion and the hydrogen yield up to 77% [1].

The state-of-the-art porous anodes also enhance the heat transfer via coupling of the reforming reactions of the fuel and the electrochemical reactions within the porous matrix. However, the endothermic reforming reactions and the exothermic electrochemical reactions may cause significant temperature gradients in the anodes.

The experimental measurements [2] indicate that temperature of the surface of anodes may exceed the temperature of the inlet fuel up to 120 $K$. The increase of temperature loads on the anodes may have a significant effect on the integrity of interfaces within a fuel cell and thus result in significant performance degradation [3]. Measurements within reforming porous anodes are extremely difficult to perform thus, understanding of the heat transport in SOFC anodes requires a development of mathematical models and numerical simulations of the coupled electrochemical reactions.

Existing numerical simulations [4]–[6] of three dimensional reactive flow in SOFCs relay on the assumption that the electrochemical reactions occur only on the surface of the solid electrolyte layer. Thus, the models neglect the electrochemical charge transfer on the three-phase boundary ($TPB$) formed by the particles which compose the porous anodes. In the simulations, the transport of the electrical charge is modeled using equivalent electrical circuits, and the Ohm law for total current passing through the cell.

A motivation of the presented study was to develop a model of heat transport which extends treatment of the electrochemical reactions onto the three-phase boundary within the anodes. A goal was to conduct numerical simulations of the temperature distribution in the anodes of a button SOFC. Unlike the models of reforming anodes reported in the literature, the present approach simulates the heat transport based on three-dimensional distribution of the electrical field in the anode porous matrix. Also in our model, all thermodynamic parameters are implemented as polynomial functions of temperature of the fuel.

The calculations were conducted to simulate the reforming anode in a button SOFC (see schematic in Fig.1) which was investigated in the experiments [7]. The results of the experiments are considered to be a reliable data for the validation of the SOFC numerical models reported in literature [8]. The anode of the cell was composed of porous Ni/YSZ cermet. The cell diameter was 2 $cm$, and thickness of the anode was 0.5 $cm$. In the experiments, methane with 3 $wt\%$ of water steam was used as a fuel. The electrical current was varied up to 2 $A/cm^2$.

## 2 MODEL DEVELOPMENT

### 2.1 Reforming and Electrochemical Reactions

Internal reforming of methane and carbon monoxide can be described by the following reactions [9]:

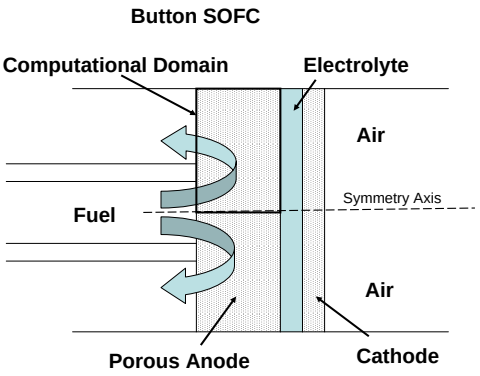


Figure 1: Schematic of SOFC cross section.

$$CH_4 + H_2O \leftrightarrow CO + 3H_2 \quad (1)$$

$$CO + H_2O \leftrightarrow CO_2 + H_2 \quad (2)$$

Water-gas shift reaction (1) is endothermic and requires heat influx generated by the electrochemical reactions. Electricity is generated by the oxidation of hydrogen and carbon monoxide:

$$H_2 + O^{2-} \leftrightarrow H_2O + 2e^- \quad (3)$$

$$CO + O^{2-} \leftrightarrow CO_2 + 2e^- \quad (4)$$

In the simulation, reforming and electrochemical reactions is assumed to occur within the porous layer of the anode. Thermal equilibrium between the fuel components and the solid matrix of the anode is specified in the model.

## 2.2 Governing Equations of Fuel Flow

The governing equations for the gas mixture are the mass balance equations for the mixture and its components, momentum (Navier-Stokes), and energy balance equations. The equations are solved for steady state flow in the three-dimensional domain representing the porous anode. The mass balance equation for the fuel is written as follows:

$$\nabla(\rho \mathbf{v}) = S_m, \quad (5)$$

where $\rho$, and $\mathbf{v}$ is density of the mixture and superficial velocity in the porous matrix respectively. Source term $S_m$ describes the mass flux due to electrochemical reactions (3) and (4) on TPB within the porous layer:

$$S_m = \big( -\frac{i_{H_2}}{2F} M_{H_2} - \frac{i_{CO}}{2F} M_{CO} + \frac{i}{2F} M_{H_2O} \big) A_s, \quad (6)$$

where $A_s$ is specific active area for the reactions, $i_{H_2}$, $i_{CO}$, and $i = (i_{H_2} + i_{CO})$ is reactant specific and total current density respectively. Molar masses of the mixture components are denoted by $M_{H_2}$, $M_{CO}$, $M_{H_2O}$, and $F$ is the Faraday constant. The momentum equation for incompressible flow reads:

$$\rho \mathbf{v} \nabla(\mathbf{v}) = -\nabla P + \nabla(\mu(\nabla \mathbf{v}) + S_D, \quad (7)$$

where $\mu$ is dynamic viscosity of the mixture, and $P$ is pressure. The momentum losses in the porous matrix are calculated using the Darcy's law:

$$S_D = -\mu \mathbf{v} / K, \quad (8)$$

where $K$ is permeability of the porous anode. The value of the permeability is determined by Kozeny-Carman formula [8]:

$$K = \frac{\varepsilon^3 d^2}{72\tau(1-\varepsilon)^2}. \quad (9)$$

The values of pore radius $d$, porosity $\varepsilon$, and tortuosity $\tau$ are specified to be the same as the data [8]. The conservation equations for the species are written as following:

$$\nabla(\rho \mathbf{v} Y_i) = \nabla(\rho D_i \nabla Y_i) + S_s i, \quad (10)$$

where $Y_i$ is mass fraction, and $D_i$ is effective diffusivity of specie $i$. The diffusivity can be calculated using Stefan-Maxwell multi-component diffusion coefficients $D_{SM,i}$ [4], and the Knudsen diffusivity $D_{K,i}$ which becomes predominant in case when free-path of molecules is comparable with the size of the pores [8]:

$$D_i = \frac{\varepsilon}{\tau} \big( \frac{D_{SM,i} \times D_{K,i}}{D_{SM,i} + D_{K,i}} \big) \quad (11)$$

$$D_{K,i} = \frac{2}{3} \frac{\varepsilon}{\tau} d \sqrt{\frac{8RT}{\pi M_i}} \quad (12)$$

$$D_{SM,i} = (1 - X_i) / (\sum_k X_k / D_{ik}), \quad (13)$$

where $D_{ik}$ are binary diffusivity of the species, and $X_i$ is molar fraction of specie $i$. The source terms in Eq. 10 include the mass fluxes due to the chemical and electrochemical reactions and are defined as following:

$$S_{s,H_2} = (3R_r + R_s) M_{H_2} - \frac{i_{H_2}}{2F} M_{H_2} A_s \quad (14)$$

$$S_{s,CH_4} = -R_r M_{CH_4} \quad (15)$$

$$S_{s,H_2O} = (-R_r - R_s) M_{H_2O} + \frac{i}{2F} M_{H_2O} A_s \quad (16)$$

$$S_{s,CO} = (R_r - R_s) M_{CO} - \frac{i_{CO}}{2F} M_{CO} A_s, \quad (17)$$

where $R_r$, and $R_s$ is reaction rate of steam reforming and water-gas shift reaction respectively. In nickel/zirconia cermet, the reaction rates vary significantly depending on the amount of catalyst and the structure of porous anode. Extensive review [9] indicates that the reaction rates can be computed using temperature dependent rates of forward and backward reactions $k^+(T)$,


Clean Technology 2008, www.ct-si.org, ISBN 978-1-4200-8502-0

$k^-(T)$, and partial pressure of the fuel components $p_i$. In this approach, the kinetics rates are approximated by the correlations which are experimentally validated for Ni/YSZ porous anodes. In the simulation, the equations reported in [9] are utilized for the computation of the reforming rates:

$$R_r = k_r^+ p_{CH_4} p_{H_2O} - k_r^- p_{CO} p_{H_2}^3 \tag{18}$$

$$R_s = k_s^+ p_{CO} p_{H_2O} - k_s^- p_{CO_2} p_{H_2}. \tag{19}$$

The energy equation balances the fluxes of heat advection, heat diffusion, viscous dissipation, and the heat net input due to the chemical and electrochemical reactions:

$$\nabla(\mathbf{v}(\rho E + p)) = \nabla\big(k_{eff}\nabla T - \sum_j h_j \mathbf{J}_j + (\tau_{eff}\mathbf{v})\big) + S_h, \tag{20}$$

where internal energy $E = h - p/\rho + v^2/2$, enthalpy of the gas mixture is defined as $h = \sum_j Y_j h_j$, and enthalpy of specie $i$ is calculated as $h_j = \int c_{p,j} dT$. Viscosity tensor $\tau_{eff}$ is specified using the law of ideal gas mixture.The heat source in Eq. 20 is associated with the chemical reactions (1), and (2):

$$S_h = \sum_i R_i \Delta h_i, \tag{21}$$

where the value of $\Delta h_i$ is specified to be equal to the reaction enthalpy of the chemical and electrochemical reactions [4]. Effective thermal conductivity $k_{eff}$ is estimated by the weighted average:

$$k_{eff} = \varepsilon k + (1-\varepsilon) k_{YSZ}, \tag{22}$$

where $k_{YSZ}$ is thermal conductivity of the cermet, and $k$ is thermal conductivity of the fuel. The latter thermal conductivity is computed using the ideal gas mixture law where the conductivity of an individual specie depends on temperature. The closure of the model requires a specification of heat capacity, thermal conductivity, dynamic viscosity and binary diffusion coefficients for every individual specie of the fuel as functions of temperature. In the simulation, we use an approximation of the parameters by the polynomials of 6-th order [12].

## 2.3 Model of Electrical Fields in Porous Anode

Electrochemical reactions (3), (4) are known to be localized near the boundary between the electron conducting particles, the ion-conducting particles and the reactant gas phase. An approximation of the zone by a mathematical surface separating electrolyte and anode is often used in the simulations of SOFCs. However, modeling of the zones as finite volumes leads to better representation of the actual transport processes in the

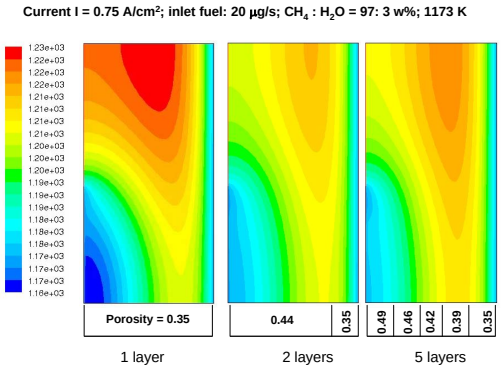


Figure 2: Temperature contours (K) in uniform (1 layer) and graded anodes (2 layers and 5 layers with average porosity 0.42)

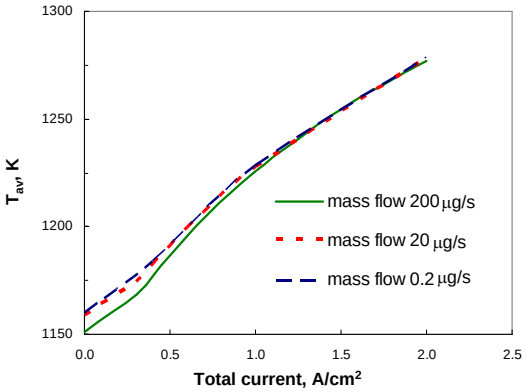


Figure 3: Avearage temperature in the uniform anode (inlet temperature 1173 K)

porous anodes. In our simulation, the electrochemical reactions are modeled as the oxidation of hydrogen and carbon monoxide which occurred on TPB within the anode.

Electronic and ionic currents are simulated solving the equations for corresponding potentials $\phi_{el/ion}$:

$$\nabla(\sigma_{el}^{eff}\nabla\phi_{el}) = R_{BV} \tag{23}$$

$$\nabla(\sigma_{ion}^{eff}\nabla\phi_{ion}) = -R_{BV} \tag{24}$$

where $\sigma_{el/ion}^{eff}$ is the effective electron/ion conductivity of the porous anode. The equations were utilized in [14] for the simulation of SOFC with pure hydrogen as the fuel. In case of the reforming anodes, the Butler-Volmer volumetric transfer current density $R_{BV}$ has to include oxidation of carbon monoxide as an additional pathway of current transfer. Thus, the Butler-Volmer density depends on activation polarizations $\eta_{H_2}$ and $\eta_{CO}$ associated with reactions (3) and (4) respectively. In our simulation, the transfer current density is calculated as $R_{BV} = R_{BV}^{H_2} + R_{BV}^{CO}$, where each term in the right side of the equation is specified using the Butler-Volmer equa-

tion shown in [14]. Identification of the multiple reaction pathways remains a topic of ongoing theoretical analysis [10] and requires new experimental data. In our model, we suggest to close the set of the governing equations using the resistance correlations for the activation polarization reported in [11]. The correlations were derived from the measurements of total current density and average polarization in the reforming anodes. In the simulation, we assume that these correlations can be utilized to calculate local activation polarization $\eta$ as the function of local current density $i = \sigma_{el}^{eff} |\nabla \phi_{el}|$:

$$\eta_k = r_k \; exp(E_k/T) i, \;\; k = H_2, CO \qquad (25)$$

where $r_i$ and $E_i$ are the empirical parameters [11].

## 3 Simulation of Uniform and Graded Anodes

The model is implemented using CFD package *Fluent* and is applied for simulations of the uniform and the graded anodes. In the latter case, the anode is assumed to be composed of two or five layers with different porosities. The grading is considered to optimize the gas transport through the anode [13]. The results of the simulation (see Fig.2 to 6) indicate that the graded anodes may improve the overall performance of SOFCs and decrease temperature gradients within the anodes.

## REFERENCES


[1] N.Hotz, et al., J Power Sources, 158(1), 333-347, 2006.
[2] Z. Shao, et al., Solid State Ionics, 175, 3946, 2004.
[3] D. Waldbilliga, et al., Solid State Ionics, 176, 847859, 2005.
[4] J. Yan, et al., J Fuel Cell Science and Technology, 3, 89-98, 2006.
[5] S. Cordiner, et al., Applied Thermal Engineering, 27, 738-747, 2006.
[6] Y. Hao, et al., J Electrochemical Society, 154(2), B207-B217, 2007.
[7] Y. Liu, et al., Solid State Ionics, 158, 11-16, 2003.
[8] V. Janardhanan, et al., J Power Sources, 162, 1192-1202, 2006.
[9] B. Haberman, et al., Int J Heat Mass Transfer, 47, 3617-3629, 2004.
[10] W. Bessler, et al., Solid State Ionics, 177, 3671-3383, 2007.
[11] E. Hernandez-Pacheco, et al., J Power Sources, 138, 174-186, 2004.
[12] B. Todd, et al., J Power Sources, 110, 186-200, 2002.
[13] P. Holtappels, et al., Fuel Cells, 2, 113-116, 2006.
[14] M. Hussain, et al., J Power Sources, 161, 1012-1022, 2006.


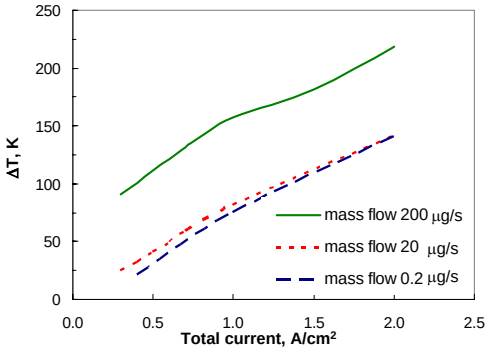


Figure 4: Difference between maximum and minimum temperature in the uniform anode (inlet temperature 1173 K)

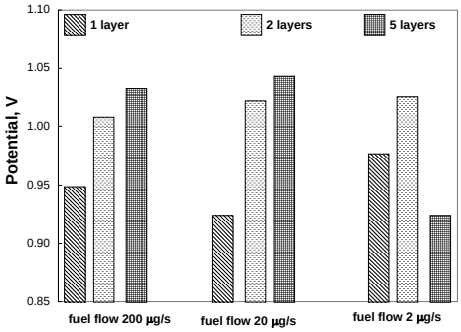


Figure 5: Nernst cell potential (current density 0.75 $A/cm^2$)

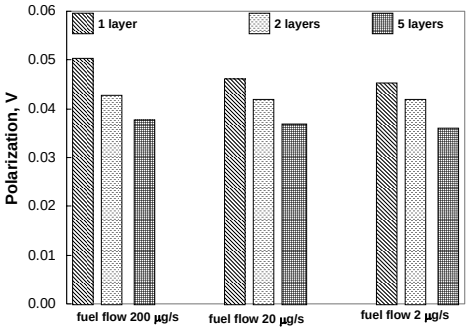


Figure 6: Average activation polarization in the anodes (current density 0.75 $A/cm^2$)